Bull. Mater. Sci., Vol. 36, No. 1, February 2013, pp. 37–44. © Indian Academy of Sciences.

Effect of different carbon fillers and dopant acids on electrical properties of polyaniline nanocomposites

E JOHNY JELMY, S RAMAKRISHNAN, MURALI RANGARAJAN and NIKHIL K KOTHURKAR*

Department of Chemical Engineering and Materials Science, Amrita Vishwa Vidyapeetham, Coimbatore 641 112, India

MS received 20 October 2011; revised 17 April 2012

Abstract. **Electrically conducting nanocomposites of polyaniline (PANI) with carbon-based fillers have evinced considerable interest for various applications such as rechargeable batteries, microelectronics, sensors, electrochromic displays and light-emitting and photovoltaic devices. The nature of both the carbon filler and the dopant acid can significantly influence the conductivity of these nanocomposites. This paper describes the effects of carbon fillers like carbon black (CB), graphite (GR) and muti-walled carbon nanotubes (MWCNT) and of dopant acids like methane sulfonic acid (MSA), camphor sulfonic acid (CSA), hydrochloric acid (HCl) and sulfuric acid (H_2SO_4) on the electrical conductivity of PANI. The morphological, structural and electrical properties of neat PANI and carbon–PANI nanocomposites were studied using scanning electron microscopy (SEM), Fourier transform infrared spectroscopy (FT–IR), UV–Vis spectroscopy and the four-point probe technique, respectively. Thermogravimetric analysis (TGA) and X-ray diffraction (XRD) studies were also conducted for different PANI composites. The results show that PANI and carbon–PANI composites with organic acid dopants show good thermal stability and higher electrical conductivity than those with inorganic acid dopants. Also, carbon–PANI composites generally show higher electrical conductivity than neat PANI, with highest conductivities for PANI–CNT composites. Thus, in essence, PANI–CNT composites prepared using organic acid dopants are most suitable for conducting applications.**

Keywords. **Polyaniline; dopant; electrical conductivity; carbon nanotubes.**

1. Introduction

Intrinsically conducting polymers (ICPs) have potential applications in many areas such as electrochemistry, electromagnetic systems, electronics, electromechanical systems, electroluminescence and sensors. Polyaniline is one of the most important conducting polymers due to its relatively facile synthesis, electrical conductivity and environmental stability (Feast *et al* 1996; Syed and Dinesan 1991). The electrical conductivity of polyaniline depends mainly on the dopant acid concentration, oxidant-to-monomer ratio (OM ratio), rate of addition of oxidant to the monomer, temperature of the reaction medium, nature of dopant acids, purity of monomer and polymerization time (Pron *et al* 1988; Syed and Dinesan 1991; Cortes and Sierra 2006). Out of these, the type of dopant acid is an important factor deciding the conductivity and thermal stability of polyaniline (Kulkarni *et al* 1989; Kahol *et al* 2003) and its composites. Generally, inorganic acids are used as doping agents but, unfortunately polyaniline doped with inorganic acids are neither soluble nor fusible (Levon *et al* 1995; Sinha *et al* 2009). Methane sulfonic acid (MSA), camphor sulfonic acid (CSA) and dodecyl benzene sulfonic acid (DBSA) are some of the commonly used organic dopants. The $–SO_3H$ group in these acids allows protonation of aniline during polymerization. Recent studies have shown that the introduction of multi-walled carbon nanotubes (MWCNTs) in polyaniline enhances the electrical properties by facilitating charge-transfer processes between the two components (Cochet *et al* 2001; Maser *et al* 2003; Bhadra *et al* 2009). Nanocomposites of nanotubes with different polymers have been prepared using several methods such as melt mixing, *in situ* polymerization, grafting macromolecules to the CNTs, and electrochemically (Saraswathi and Gajendran 2008). The present study investigates the effect of different dopant acids on the electrical conductivity of PANI and the effect of different carbon fillers and dopant acids on the electrical conductivity of PANI–carbon composites. PANI was synthesized by chemical polymerization of aniline in different acids, viz. MSA, CSA, HCl and H_2SO_4. The structures of different dopant acids used are given in figure 1. The PANI–carbon composites were synthesized *in situ* by adding different forms of carbon, viz. CB, GR and MWCNT during PANI synthesis.

2. Experimental

2.1 *Materials and methods*

2.1a *Materials*: Laboratory grade aniline, D-10 camphor sulfonic acid (CSA), methane sulfonic acid (MSA),

*Author for correspondence (nikhil.kothurkar@gmail.com)

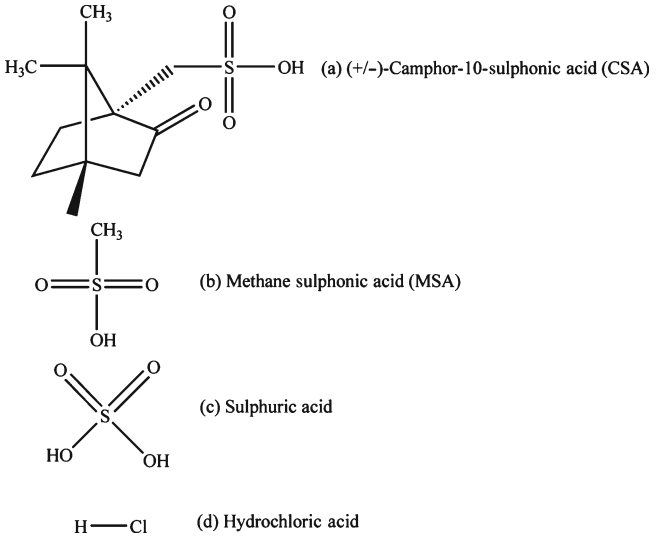

Figure 1. Structures of different dopants used.

hydrochloric acid (HCl), sulfuric acid (H_2SO_4), ammonium persulphate $(NH_4)_2S_2O_8$ (APS), hydrogen peroxide and dimethyl sulphoxide (DMSO) were procured from Merck India. Aniline was distilled under vacuum and stored below 4 °C. MWCNTs were received from Yunnan Great China. Graphite (GR) powder and carbon black (CB) were received from Loba Chemicals.

2.1b *Preparation of graphite nanosheets*: Expandable graphite powders were prepared using H_2O_2–H_2SO_4 as follows (Du *et al* 2004; Nikzad *et al* 2009). A mixture of concentrated sulfuric acid and hydrogen peroxide (1:0·08 volume ratio) was mixed with graphite powder. The mixture was stirred at an ambient temperature for about 1 h. The as-treated graphite was washed with distilled water thrice and dried at 100 °C for 24 h in a hot air oven in order to obtain the expandable graphite powders. The exfoliation was done by ultrasonication. The expanded graphite powders were dispersed in distilled water and then sonicated for 10 h at room temperature. The graphite nanosheets were filtered (Whatman No. 40), washed with distilled water and then dried under vacuum at 50 °C.

2.1c *In situ polymerization to prepare polyaniline carbon composites*: PANI–carbon composites were synthesized by *in situ* chemical oxidative polymerization of aniline in the presence of dopant acid, APS and the carbon filler (Zengin *et al* 2002; Du *et al* 2004; Reddy *et al* 2009). For composite preparation, a solution of 0·25 M dopant acid (20 ml) containing the filler (approximately 10 wt% of the monomer) was sonicated at room temperature for three days to get a good suspension. This solution was mixed with aniline in dopant acid (0·25 M) in a round-bottom (RB) flask which was maintained at a temperature around 0–2 °C with continuous stirring. To this cold solution, 0·25 M aqueous ammonium persulfate solution (62·5 ml) was added in drops over a period of 2 h. In all the syntheses, the aniline to dopant volume ratio was kept constant as 1:50 and the oxidant to monomer ratio as 1. After constant stirring for 24 h, the formed polymer composite was vacuum filtered and washed with 250 ml of acid solution containing the same concentration of dopant (acid) to remove the unreacted oligomers and monomers. The residue remaining in the filter paper was then dried at 60 °C for 24 h to obtain dark greenish PANI–MWCNT (PCNT) composites. Neat PANI without the filler was also synthesized using different dopants. Further, PANI composites were made in MSA with different forms of carbon-like CB, exfoliated GR and MWCNTs. The details of the prepared samples are described in table 1.

Table 1. Details of samples prepared.

Sample name	Dopant acid	Carbon filler
P–MSA	MSA	Nil
P–CSA	CSA	Nil
P–HCl	HCl	Nil
P–H_2SO_4	H_2SO_4	Nil
PCNT–MSA	MSA	MWCNT
PCNT–CSA	CSA	MWCNT
PCNT–HCl	HCl	MWCNT
PCNT–H_2SO_4	H_2SO_4	MWCNT
PCB–MSA	MSA	CB
PGR–MSA	MSA	GR

2.2 *Characterization*

The UV–Visible spectra of the PANI and its nanocomposites were recorded at an ambient temperature using a Varian, Cary 5000 UV-Vis-NIR spectrometer. The absorption spectra of dilute solutions of PANI and PCNT in DMSO (∼0·25 mg/mL) were recorded in the wavelength range of 300–1000 nm. Fourier transform infrared (FT–IR) spectra were recorded on a Thermo Nicolet, iS10 FT–IR spectrometer using KBr pellets in the range of 500–4000 cm^{-1}. A multi-point base line correction was made for all the FTIR spectra and the corrected peak areas were determined using OMNIC 8.1 software. The ratios of peak areas of quinoid to benzoid peaks (A_Q/A_B), $–NH^+$ = stretch to quinoid peak ($A_{-NH+=}/A_Q$) and $–NH^+$ = stretch to benzoid peak ($A_{-NH+=}/A_B$) for different composites were calculated for each sample. The morphology of the nanocomposites was examined using a JEOL JSM-5600 LV field emission scanning electron microscope (FE–SEM). For the conductivity measurements, pellets of 13 mm diameter and 3 mm thickness were prepared using a hydraulic press (6 ton force for 2 min). Conductivity measurements were made on the pellets (2 replicates) using a four-point probe with a d.c. and a.c. current source (Model 6221) and a nanovoltmeter (Model 2182A) from Keithley instruments. The thermal stability was measured using a thermogravimetric analyser (Mettler Toledo TGA/SDTA 851e) in the range of

25 to 700 °C at a heating rate of 10 °C min^{-1} under nitrogen. Crystalline and amorphous structure identification of polyaniline samples were performed using X-ray diffraction (Brucker AXD D8 Advance, vertical configuration) using Cu Kα_1 radiation ($\lambda = 1{\cdot}54056$ Å).

3. Results and discussion

3.1 *UV-Vis spectroscopy*

UV–Visible spectroscopy was used to characterize the chemical structures of PANI and PCNT composites synthesized in different dopant acids. Figure 2 shows UV-Vis spectra of PCNT composites in DMSO, synthesized in the presence of different dopant acids. The characteristic absorption peaks observed for PANI and PCNT composites were around 330 nm, 440 nm and a broad peak in 600–850 nm range. The band in the vicinity of 330 nm indicates the π–π^* transition of the benzene rings in the polymer backbone and the band around 440, 615 and 830 nm indicates the polaron/bipolaron transitions in doped polyaniline (Fu and Weiss 1997; Koul *et al* 2000; Ghosh *et al* 2001; Bitao Su *et al* 2007; Kapil *et al* 2009). The peak at 330 nm was shifted to higher wavelengths for the samples with organic dopant acids. This indicates a lower energy for the π–π^* electronic transitions, due to the extended conjugation length in the system. A correlation has been observed in the literature between this band and room temperature electrical conductivity of PANI (MacDiarmid *et al* 1995). In our PCNT composite samples, the polaron/bipolaron transition was red shifted when the dopants used were organic dopants as compared to inorganic acids. Therefore, PANI samples with an organic dopant acid are expected to have higher electrical conductivity.

Figure 3 shows absorption spectra of P–CSA and PCNT–CSA. The peak at 326 nm in P–CSA is shifted to 309 nm in PCNT–CSA composites. Such a hypsochromic shift of the π–π^* band in PCNT compared to PANI has been reported in the literature (Gopalan *et al* 2007; Jeevananda *et al* 2008) and it has been suggested to be due to the site-selective interaction between the quinoid ring of the PANI and CNTs (Cochet *et al* 2001). When PANI coats over the CNTs, the interfacial interaction between the two causes the π–π^* transition to shift to a lower wavelength (Ghatak *et al* 2010). But at the same time, the absorption peak due to the polaron/bipolaron transition was red shifted in PCNT compared to neat PANI. Thus one can expect a higher electrical conductivity for the PCNT composites as compared to neat PANI.

3.2 *FT–IR spectra analysis*

To further identify the structural features, FT–IR analysis of PANI and its composites was performed. Figure 4 shows FT–IR spectra of composites of PANI with different forms of carbon. The FT–IR spectra of all composites have characteristic peaks around 1580 cm^{-1} (quinoid ring stretch), 1480 cm^{-1} (benzoid ring stretch), 1294 cm^{-1} (N–H bend), 1240 cm^{-1} (asymmetric C–N stretch), 1110 cm^{-1} (–NH^+= stretch) and 790 cm^{-1} (aromatic C–H ring bend). The peak

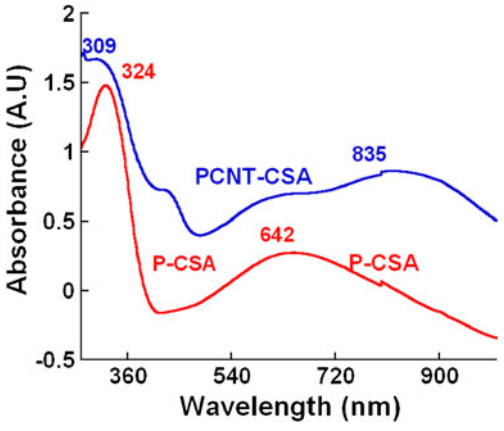

Figure 3. UV-Vis spectra of PANI and PCNT composite synthesized using CSA.

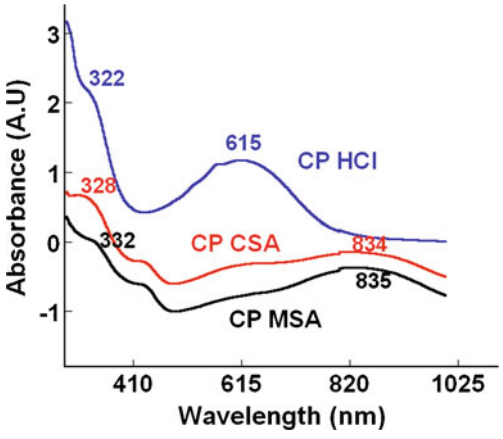

Figure 2. UV-Vis spectra of PCNT composites synthesized in presence of different dopants.

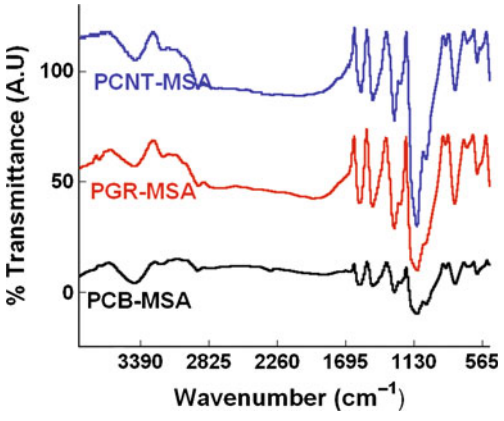

Figure 4. FT–IR spectra of PANI–carbon composites using different carbon fillers.

Table 2. Ratios of area of different peaks in FTIR spectra.

Samples	A_Q/A_B	$A_{NH+=}/A_Q$	$A_{NH+=}/A_B$
P–MSA	0·93	5·23	4·85
PCNT–MSA	1·15	10·05	11·60
PGR–MSA	1·04	6·57	6·82
PCB–MSA	1·01	6·93	7·02

around 790 cm^{-1} is the characteristic of para-substituted aromatic ring, through which the polymerization is expected to progress. The presence of the quinoid and benzoid peaks reveals that the polymer is made out of both amine and imine groups (indicating that the polymer is the conductive emeraldine salt form of PANI). The strong band at 1110 cm^{-1} was described by MacDiarmid (Chiang and MacDiarmid 1986; Zengin *et al* 2002) to be a measure of the degree of delocalization of electrons and is also indicative of high conductivity. The $-NH^+=$ stretch peak positions for PCNT–MSA, PGR–MSA and PCB–MSA were 1110, 1108, 1104 cm^{-1}, respectively. The peak for the PCNT–MSA composite is thus blue shifted compared to the other two and is also much narrower. This indicates some interaction between CNTs and PANI.

To further investigate the correlation between the area of the $–NH^+$ = peak (~1110 cm^{-1}) and the conductivity of the composites, the peak areas for the quinoid, benzoid and the $–NH^+=$ peaks were calculated and their ratios compared (table 2). The A_Q/A_B ratios for PCNT–MSA, PGR–MSA, PCB–MSA were nearly identical indicating that different fillers do not change the oxidation form of PANI. However, the PCNT–MSA composite showed a relatively larger $A_{-NH+=}/A_Q$ ratio compared to the other two. A similar trend was observed for the $A_{-NH+=}/A_B$ ratio. This clearly shows that compared to the benzoid or quinoid peaks, the $-NH^+=$ peak is significantly enhanced in PCNT–MSA. As such, a greater conductivity is expected for this composite as per the literature (Chiang and MacDiarmid 1986; Zengin *et al* 2002).

The $–NH^+=$ stretch peak positions for PCNT–MSA, and P–MSA were 1156, 1110 cm^{-1}, respectively. The peak for the P–MSA composite is thus blue shifted compared to PCNT–MSA (Zengin *et al* 2002; Gopalan *et al* 2007). This may be due to the interaction between CNTs and PANI (Cochet *et al* 2001). Additionally, an enhancement in the $-NH^+=$ peak was observed in PCNT–MSA compared to the neat polymer P–MSA (figure 5). The value of $A_{-NH+=}/A_Q$ was higher in PCNT–MSA as compared to P–MSA. This enhancement in peak area is indicative of charge transfer between PANI and CNT.

3.3 *Morphology analysis of polymer composites*

Figure 6 shows SEM image of PANI–carbon composites. The SEM image of PCNT–MSA composite (figures 6a and b) shows the presence of CNTs coated with PANI. The sorption of the aniline monomer on CNTs is possible because of its high surface area (Saini *et al* 2009). The sorbed monomer then polymerizes to form PANI-coated CNTs. This morphology facilitates electron transfer throughout the composite, which results in high electrical conductivity. Figure 6(c and d) shows the SEM micrograph of PGR composite. The image shows the partially exfoliated graphite layers and the presence of PANI on the surface of graphite. The exfoliation process was incomplete probably due to the inadequate sonication during the process. The main reason for exfoliating the graphite is to allow PANI in between the graphite layers so as to produce conductive composites. Figure 6(e) shows the SEM image of PCB–MSA composite. With the incorporation of CB (10 wt%), the composites show a globular agglomerated morphology. Polymerization of aniline is expected to take place on the surface of dispersed CB particles and thus the composite has a globular morphology (Reddy *et al* 2009).

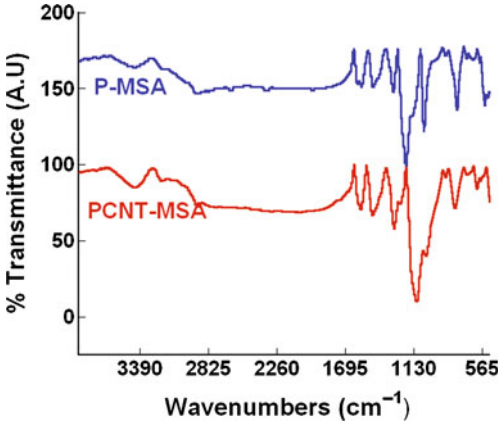

Figure 5. FT–IR spectra of PANI and PCNT composites synthesized using MSA.

3.4 *Electrical conductivity*

The electrical conductivity of PANI and PANI–nanocomposite samples at room temperature was measured using a four-point probe method. The d.c. conductivity results are given in table 3. Both the dopant acid and the type of carbon filler significantly influence the conductivity. The use of organic dopants was found to increase the conductivity of PANI and PCNT composites. The conductivities for PANI and PCNT composites in different dopant acids are shown in figure 7. The enhanced conductivity is due to the dopant effect (Bourdo and Viswanathan 2005) whereby dopants with a sulfonate counter ion capable of hydrogen bonding, can give samples with better d.c. conductivity (Hopkins *et al* 1996). So for high-conducting applications, organic dopants are preferable to inorganic acid dopants. Figure 8 shows conductivities of PANI–carbon nanocomposites with different carbon fillers. PCNT composites exhibit higher conductivity compared to composites with other

fillers, for the same dopant acid. The sorption of the aniline monomer on the surface of CNTs leads to the formation of a PANI-coated CNT morphology. CNTs are relatively good electron acceptors while PANI may be considered to be a good electron donor (Zengin *et al* 2002). This can facilitate the π–π^* interaction between the surface of CNT and the quinoid rings of polyaniline. The monomer sorption by the filler is higher in CNTs due to their high surface area

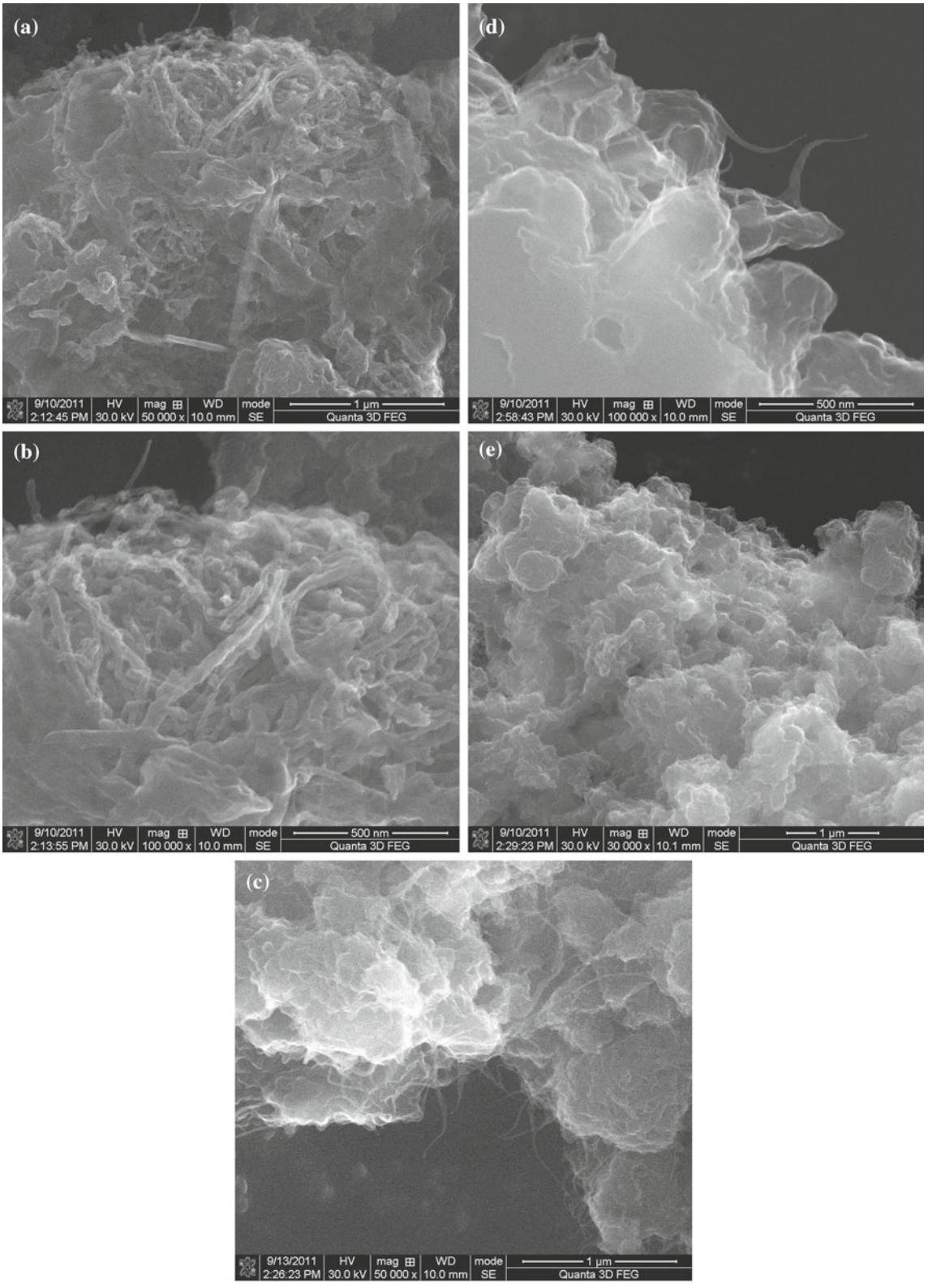

Figure 6. SEM images of (**a**) PCNT–MSA, (**b**) PGR–MSA, (**c**), (**d**) and (**e**) PCB–MSA composites.

Table 3. D.C. electrical conductivity values for various samples.

Sample type	Conductivity (S/cm)
P–H_2SO_4	0·007
P–HCl	0·009
P–MSA	0·015
P–CSA	0·016
PCB	0·03
PGR	0·07
PCNT–H_2SO_4	2·28
PCNT–HCl	3·02
PCNT–MSA	6·48
PCNT–CSA	7·58

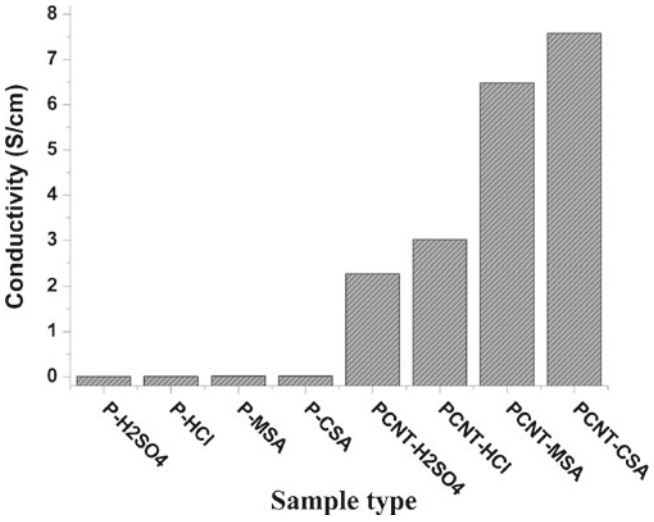

Figure 7. D.C. electrical conductivities of PANI and PCNT composites with different dopants.

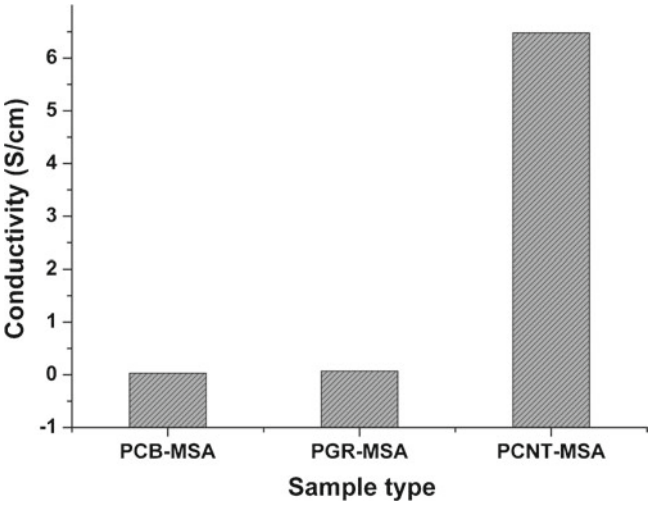

Figure 8. D.C. electrical conductivities of PANI composites with different types of carbon forms.

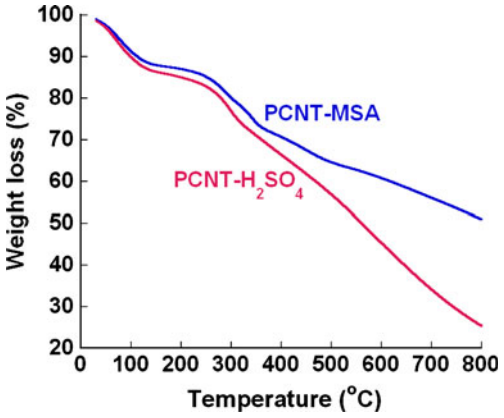

Figure 9. TGA curves of PCNT with different dopants.

compared to CB and GR. This morphology should reduce the interfacial resistance between the CNTs and the matrix, thus enabling better electron transfer in PCNT–MSA composites compared to PCB–MSA and PGR–MSA. Thus the observed electrical conductivity trends are consistent with the expectations from the UV–Visible and FTIR spectroscopic results and the SEM morphological study.

3.5 *Thermogravimetric analysis (TGA)*

Figure 9 shows thermograms of PCNT–MSA and PCNT–H_2SO_4 composites. TGA curves of the composites show a nearly continuous weight loss with respect to temperature. However, three distinct weight losses could be detected (table 4). The first weight loss occurs at a temperature of ∼80–90 °C due to loss of moisture. The second loss around 210–250 °C is due to the loss of the counter anion of the dopant acid. The third weight loss around 350–400 °C is due to the degradation of the polymer backbone. A charred residue was observed after the analysis and this may be due to the presence of stable materials like MWCNTs and catalysts used for the synthesis of CNTs. For PCNT–MSA and PCNT–H_2SO_4 the weight losses were 10·4% and 12·3% at around 85 °C and 15·5% and 13·0% at around 240 °C, respectively. The weight loss of PCNT–MSA at around 240 °C (15·5%) was higher than the weight loss in PCNT–H_2SO_4 (13%), because of the bulkier counter anion of MSA. From the TG curves, we can observe that the % weight loss for PCNT–MSA was somewhat lower than PCNT–H_2SO_4 at any given temperature. This indicates that the thermal stability of PCNT–MSA compared to PCNT–H_2SO_4 is comparable or slightly better. Literature reveals similar trends for neat PANI (Kulkarni *et al* 1989). Thus, good thermal stability coupled with high electrical conductivity is the most significant advantage of organic dopant acids for the synthesis of PANI and PCNT composites.

3.6 *X-ray diffraction analysis*

The XRD patterns of PANI–carbon composites are shown in figure 10. The characteristic reflections of doped PANi

Table 4. Details of % weight loss at different temperatures.

Sample	Loss of moisture		Loss of counter ion	
	Temperature (°C)	% Weight loss	Temperature (°C)	% Weight loss
P–H_2SO_4	80	12·3	214	13
P–MSA	84	10·4	234	15·5

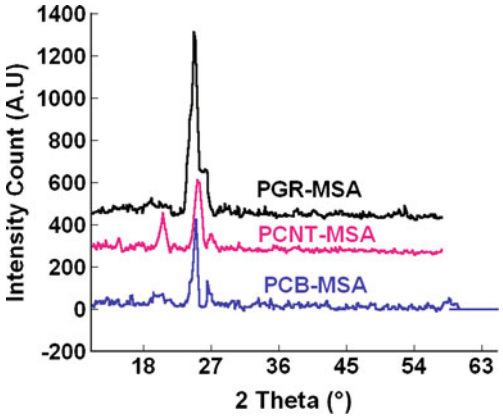

Figure 10. XRD patterns of PANI composites with different types of carbon forms.

corresponding to the (0 1 1), (0 2 0) and (2 0 0) planes are observed in the vicinity of 2θ values of 15°, 21° and 25° (Sinha *et al* 2009). The peak around $2\theta \sim 26°$ is observed in all forms of carbon composites which is due to the reflection from the (0 0 2) plane (Cochet *et al* 2001; Nikzad *et al* 2009). PCNT composite shows characteristic peaks of both PANI and CNT. The intensities of the peaks of PANI at $2\theta \sim 21°$ and 15° were very less in PCB–MSA and PGR–MSA composites compared to PCNT. This indicates a lower crystallinity of PANI in PCB–MSA and PGR–MSA compared to PCNT. Whether the higher crystallinity of PANI in PCNT was a contributory factor to the higher conductivity of PCNT compared to PCB–MSA or PGR–MSA is unclear owing to contrary findings in the literature (Liu *et al* 2002).

4. Conclusions

Conducting PANI and PANI–carbon composites were synthesized in the presence of different dopant acids (HCl, H_2SO_4, methane sulfonic acid and camphor sulfonic acid). Higher electrical conductivities were observed for all PANI–carbon composites (with different forms of carbon fillers), compared to neat PANI. The use of organic dopant acids yields PANI and its composites with better conductivity compared to those with inorganic dopants. This is attributed to the better electron transfer in the system as evidenced from UV and FT–IR analyses. Futher, thermogravimetric analysis showed good thermal stability for the composites prepared using organic dopants. The good thermal stability coupled with high electrical conductivity reveals the advantages of organic dopant acids for the synthesis of conductive PANI and PANI–carbon composites. PANI composites were prepared with MWCNTs, carbon black and graphite. The PCNT–MSA composites showed better conductivity than PCB–MSA and PGR–MSA composites. In the PCNT–MSA composites, polymerization of aniline monomer takes place on the surface of the CNTs because of its high surface area and is thought to facilitate better electron transfer in PCNT–MSA compared to PCB–MSA and PGR–MSA. Thus, we conclude that PANI–CNT composites prepared using organic dopants are more suitable for conducting applications.

Acknowledgements

This work was supported by the Defence Research and Development Organization, DRDO India.

References

Bhadra S, Khastgir D, Sinha N K and Lee J H 2009 *Prog. Polym. Sci.* **34** 783
Bourdo S E and Viswanathan T 2005 *Carbon* **43** 2983
Chiang J C and MacDiarmid A G 1986 *Synth. Met.* **13** 193
Cochet M, Maser W K, Benito A M, Callejas M A, Martinez M T, Benoit J, Schreiber J and Chauvet O 2001 *Chem. Commun.* **16** 1450
Cortes M T and Sierra E V 2006 *Polym. Bull.* **56** 37
Du X S, Xiao M and Meng Y Z 2004 *Eur. Polym. J.* **40** 1489
Feast W J, Tsibouklis J, Pouwer K L, Groenendaal L and Meijer E W 1996 *Polymer* **37** 5017
Fu Y and Weiss R A 1997 *Synth. Met.* **84** 103
Ghatak S, Chakraborty G, Meikap A K, Woods T, Babu R and Blau W J 2010 *J. Appl. Polym. Sci.* **119** 1016
Ghosh P, Siddhanta S K, Samir K S, Rejaul Haque S and Amit Chakrabarti 2001 *Synth. Met.* **123** 83
Gopalan A I, Lee K P, Santhosh P, Kim K S and Nho Y C 2007 *Compos. Sci. Technol.* **67** 900
Hopkins A R, Rasmussen P G and Basheer R A 1996 *Macromolecules* **29** 7838
Jeevananda T, Siddaramaiah, Nam Hoon Kim, Seok-Bong Heo and Jonng Hee Lee 2008 *Polym. Adv. Technol.* **19** 1754
Kahol P K, Satheesh Kumar K K, Geetha S and Trivedi D C 2003 *Synth. Met.* **139** 191
Kapil A, Taunk M and Chand S 2009 *J. Mater. Sci.: Mater. Electron.* **21** 399
Koul S, Chandra R and Dhawan S K 2000 *Polymer* **41** 9305
Kulkarni V G, Campbell L D and Mathew W R 1989 *Synth. Met.* **30** 321

Levon K, Ho K H, Zheng W Y, Laakso J, Karna T, Taka T and Osterholm J E 1995 *Polymer* **36** 2733

Liu H, Hu X B, Wang J Y and Boughton R I 2002 *Macromolecules* **35** 9414

MacDiarmid, Epstein Alan G and Arthur J 1995 *Synth. Met.* **69** 85

Maser W K *et al* 2003 *Mater. Sci. Eng.* **23** 87

Nikzad L, Alibeigi S, Vaezi M R, Yazdani B and Rahimipour M R 2009 *Chem. Eng. Technol.* **32** 861

Pron A, Genoud F, Menardo C and Nechtschein M 1988 *Synth. Met.* **24** 193

Reddy K R, Sin B C, Ryu K S, Noh J and Lee Y 2009 *Synth. Met.* **159** 1934

Saini P, Choudhary V, Sinha B P, Mathur R B and Dhawan S K 2009 *Mater. Chem. Phys.* **113** 919

Saraswathi R and Gajendran P 2008 *Pure Appl. Chem.* **80** 2377

Sinha S, Bhadra S and Khastgir D 2009 *J. Appl. Polym. Sci.* **112** 3135

Su Bitao, Tong Youngchung, Bai Jie, Lie Ziqiang, Wang Ke, Mu Hongmei and Dong Na 2007 *Indian J. Chem.* **A46** 595

Syed A A and Dinesan M K 1991 *Talanta* **38** 815

Zengin H *et al* 2002 *Adv. Mater.* **14** 1480